GPM Available Products

[As of Oct. 4, 2017]

Standard Products

Processing Level	Satellite / Instrument / Algorithm	Product [Product Identifier/ Algorithm Key*1]	Key Parameters	File coverage	Available Latest Product Version (Caveats)
1	GPM/DPR/Ku	KuPR L1B [DUB]	Received Power	GPM orbit (Gorbit*)	Ver. 05 (See: page 11~)
	GPM/DPR/Ka	KaPR L1B [DAB]	Received Power	Gorbit	Ver. 05 (See: page 11~)
	GPM/GMI	GMI L1B [G1B]	Brightness Temperature (Tb)	Gorbit	Ver. 05 (See: page 4)
	GPM/GMI	GMI L1C [G1C]	Brightness Temperature (Tb)	1 orbit	Ver. 05 (See: page 6)
	Constellation/ MWS	Constellation L1C [*2]	Inter-calibrated Brightness Temperature (Tb)	Gorbit	Ver. 05 (See: page 6)
2	GPM/DPR	KuPR L2 [DU2]	Reflectivities, 3D Precipitation	Gorbit	Ver. 05 (See: page 22~)
		KaPR L2 [DA2]	Reflectivities, 3D Precipitation	Gorbit	Ver. 05 (See: page 22~)
		DPR L2 [DD2]	Dual Frequency Retrievals, 3D precipitation	Gorbit	Ver. 05 (See: page 22~)
		SLH-DPR L2 [SLP]	Spectral latent heating	Gorbit	Ver. 05 (See: page 24~)
	GPM/GMI/GPROF	GMI L2 [GL2]	Precipitation, Total Precipitable Water	Gorbit	Ver. 05 (See: page 8~)
	GPM/DPR-GMI /COMB	DPR-GMI Comb L2 [CL2]	DPR-GMI retrieval. 3D Precipitation	Gorbit	Ver. 05 (See: page 29)
3	GPM/DPR	DPR L3 Daily (TEXT) [D3D]	Precipitation	0.1°x 0.1° Daily	Ver. 05 (See: page 19~)
		DPR L3 Daily(HDF5) [D3Q]	Precipitation	0.25° x 0.25° Daily	Ver. 05 (See: page 19~)
		DPR L3 Monthly [D3M]	Precipitation	0.25° x 0.25° Monthly	Ver. 05 (See: page 19~)
		SLH-DPR L3 Gridded orbit [SLG]	Spectral latent heating	0.5°x 0.5° Gorbit	Ver. 05 (See: page 24~)
		SLH-DPR L3 Monthly [SLM]	Spectral latent heating	0.5°x 0.5° Monthly	Ver. 05 (See: page 24~)
	GPM/GMI/GPROF	GMI L3 Monthly [GL3]	Precipitation	0.25° x 0.25° Monthly	Ver. 05 (See: page 8~)
	GPM/DPR-GMI /COMB	DPR-GMI Comb L3 [CL3]	Precipitation	0.25° x 0.25° Monthly	Ver. 05 (See: page 29)
		DPR-GMI CSH L3 [CSG]	Gridded Orbital Convective Stratiform Heating	0.25° x 0.25° Gorbit	Ver. 05 (See: page 34)
		DPR-GMI CSH L3 [CSM]	Monthly Convective Stratiform Heating	0.25° x 0.25° Monthly	Ver. 05 (See: page 34)
	Multi/Multi/GSMaP	GSMaP Hourly (TEXT) [MCT]	Precipitation *3	0.1°x 0.1° Hourly	Ver. 04 (See: page 26~)
		GSMaP Hourly (HDF5) [MCH]	Precipitation *3	0.1°x 0.1° Hourly	Ver. 04 (See: page 26~)
		GSMaP Monthly [MCM]	Precipitation *3	0.1°x 0.1° Monthly	Ver. 04 (See: page 26~)

* Gorbit is the GPM orbit calculated from the southern most point back to the southern most point

GPM Available Products

[As of Oct. 4, 2017]

Near Real-Time Products (Near real-time data can be downloaded using SFTP after G-Portal user registration and public key authentication SFTP directory tree is shown in page 3. *4)

Processing Level	Satellite / Instrument / Algorithm	Product [Product Identifier/ Algorithm Key*1]	Key Parameters	File coverage	Available Product Version
1R	GPM/DPR/Ku	KuPR L1B [DUB]	Received Power	30 min	Ver. 05 (See: page 11~)
	GPM/DPR/Ka	KaPR L1B [DAB]	Received Power	30 min	Ver. 05 (See: page 11~)
	GPM/GMI	GMI L1B [G1B]	Brightness Temperature (Tb)	5 min	Ver. 05 (See: page 4)
	GPM/GMI	GMI L1C [G1C]	Brightness Temperature (Tb)	5 min	Ver. 05 (See: page 6)
	Constellation/MWS	Constellation L1C [*2]	Inter-calibrated Tb	-	Ver. 05 (See: page 6)
2R	GPM/DPR	KuPR L2 [DU2]	Reflectivities, 3D Precipitation	30 min	Ver. 05 (See: page 22~)
		KaPR L2 [DA2]	Reflectivities, 3D Precipitation	30 min	Ver. 05 (See: page 22~)
		DPR L2 [DD2]	Dual Frequency Retrievals, 3D precipitation	30 min	Ver. 05 (See: page 22~)
	GPM/GMI/GPROF	GMI L2 [GL2]	Precipitation, Total Precipitable Water	5 min	Ver. 05 (See: page 8~)
	GPM/DPR-GMI /COMB	DPR-GMI Comb L2 [CL2]	DPR-GMI retrieval. 3D Precipitation	30 min	Ver. 05 (See: page 29)
3R	Multi/Multi/GSMaP	GSMaP Hourly (HDF5) [MFW]	Precipitation *3	0.1°x 0.1° Hourly	Ver. 04 (See: page 26~)
		GSMaP Hourly (TEXT) [MFT]	Precipitation *3	0.1°x 0.1° Hourly	Ver. 04 (See: page 26~)

Auxiliary Products

Processing Level	Satellite / Instrument / Algorithm	Product [Product Identifier/ Algorithm Key*1]	Key Parameters	File coverage	Available Latest Product Version
AUX.	Auxiliary Data (JMA/GANAL)	Environmental data extracted KuPR swath [DU2/ENV]	Temperature, Air Pressure, Cloud Water Vapor, Liquid Water	Gorbit	Ver. 05
		Environmental data extracted KaPR swath [DA2/ENV]	Temperature, Air Pressure, Cloud Water Vapor, Liquid Water	Gorbit	Ver. 05
		Environmental data extracted DPR swath [DD2/ENV]	Temperature, Air Pressure, Cloud Water Vapor, Liquid Water	Gorbit	Ver. 05

GPM Available Products

[As of Oct. 4, 2017]

Notes

*1 File Naming Convention

GPM product file naming conventions is as below, and algorithm key is corresponding to (7).

GPMxxx _ sss _ YYMMDDhhmm _ hhmm _ nnnnnn _ LLS _ aaa _ VVv . h5

(1)Mission ID
(2) Sensor ID
(3) Scene Start
(4) Scene End
(5) Orbit Number — *skip for NRT data*
(6) Process Level
(7)Algorithm Key — *indicated in product list and below note (*2) for L1C*
(8)Product Version

start and end time for L3 product
hourly file: YYMMDDhhmm_H
daily file: YYMMDD_D
monthly file: YYMM_M

*2 Product Identifier for Constellation L1C

Satellite	Instrument	Product Identifier / Algorithm Key
Megha Tropiques	SAPHIR	SPH
GCOM-W	AMSR2	AM2
DMSP F16	SSMIS	MIS
DMSP F17	SSMIS	MIS
DMSP F18	SSMIS	MIS
DMSP F19	SSMIS	MIS
NOAA-18	MHS	MHS
NOAA-19	MHS	MHS
NPP	ATMS	ATS
METOP-A	MHS	MHS
METOP-B	MHS	MHS
METOP-C	MHS	MHS
TRMM	TMI	TMI

*3 Introduced satellite/instrument data in GSMaP

Term	Satellite / Instrument
2014.3.1~2014.3.4	TRMM/TMI DMSP-F16/SSMIS DMSP-F17/SSMIS DMSP-F18/SSMIS GCOM-W/AMSR2 METOP-A/AMSU-A, MHS METOP-B/AMSU-A, MHS NOAA-18/AMSU-A, MHS NOAA-19/AMSU-A, MHS
2014.3.4~	GPM/GMI (No data during Oct.22-24,2014) TRMM/TMI (No data from Apr.8,2015 onward) DMSP-F16/SSMIS DMSP-F17/SSMIS DMSP-F18/SSMIS DMSP-F19/SSMIS (No data from Feb.11,2016 onward) GCOM-W/AMSR2 METOP-A/AMSU-A, MHS * (No MHS data from Mar.27 to May 20, 2014) METOP-B/AMSU-A, MHS NOAA-18/AMSU-A, MHS NOAA-19/AMSU-A, MHS

*4 G-Portal SFTP directory tree

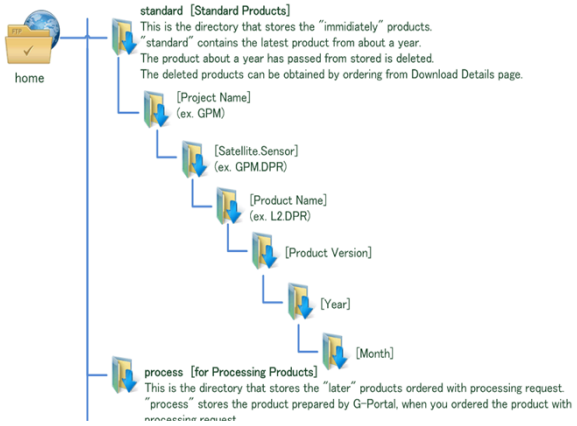

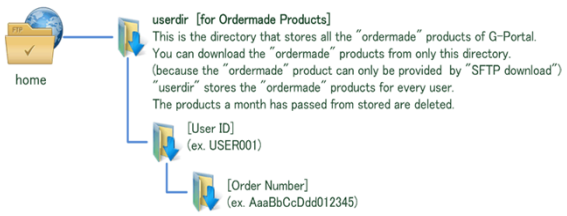

RELEASE NOTES OF GPM VERSION 05 GMI CALIBRATION

The PPS V05 GMI calibration updates include adjustments of spillover coefficients for all GMI channels (these have a major impact on T_b) and a number of other minor adjustment described below. The magnitudes of T_b changes can be seen in Figure 12.1. The T_bs are reduced around 1 K at T_b around 280 K for channels 1-5. These changes are dominated by antenna pattern correction (APC) revisions. T_b changes for other channels are minor.

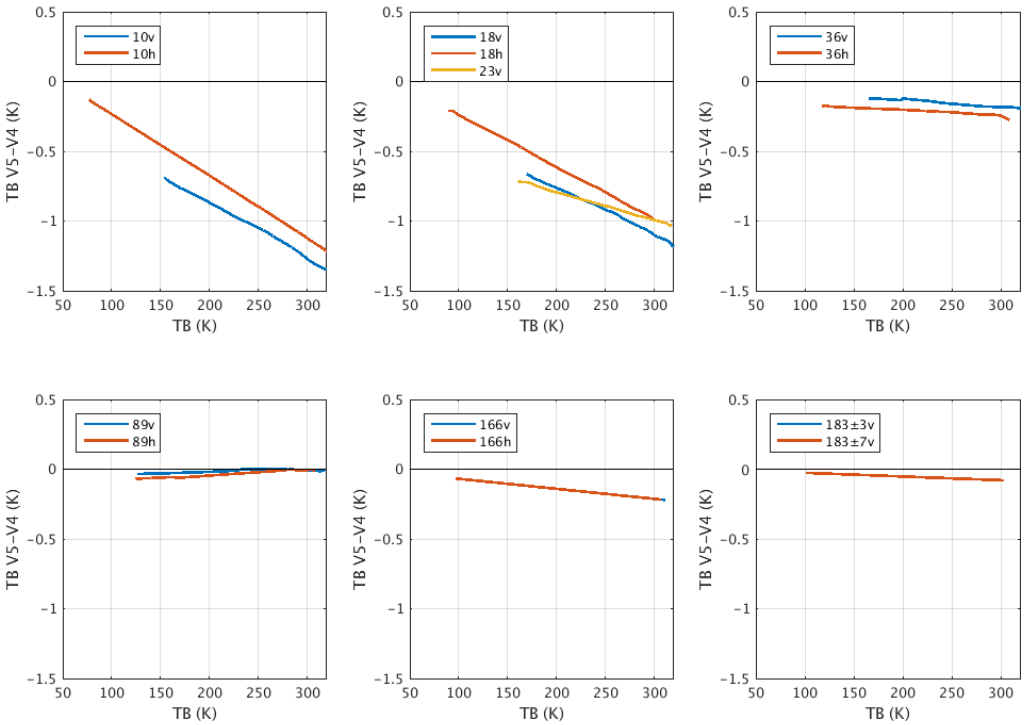

Figure 1. GMI T_b changes from V04 to V05.

1. Adjusted spillover coefficients of all GMI channels. This adjustment is the major improvement from V04 to V05 in GMI antenna pattern correction. The adjustment of spillover is based on the data from GMI deep space maneuver, inertial hold, and refinements of the analysis performed by the GMI manufacturer and the GPM Inter-calibration Working Group (X-CAL). T_b changes vary from channel to channel and are functions of brightness temperatures. For channels 1-5, the maximum change is around -1.0 K. for other channels, Tb changes are minor.

2. Adjusted cold load temperature for 10 GHz channels (from 2.74 K to 2.94 K). This is a minor adjustment and may result in T_b changes of less than 0.2 K for 10 GHz channels.

3. Added a count (earth and cold) adjustment in the magnetism correction equation. This is a minor adjustment and may result in T_b changes of less than 0.2 K.

4. Adjusted magnetic correction coefficients. This is also a minor adjustment and may result in T_b changes of less than 0.2 K.

5. Added Earth-view antenna-induced along-scan corrections (Table see ATBD Table 12.6). The correction is < 0.1 K for most pixels along a scan but can be as large as 0.5 near the edge of scans.

All of these corrections are implemented in V05 GMI L1B/Base and in ITE101.

Level 1C Version 05 (V05) Release Notes

This Level 1C V05 release involves the following changes from the previous release in the calibration of the GPM radiometer constellation.

1. Level 1C GMI V05 brightness temperature (Tc) differs from V04 by as much as -1.4 K for some channels (Figure 1) due to the following calibration adjustments implemented in V05 GMI L1B/Base:

- Adjusted spillover coefficients. This adjustment is based on the data from GMI deep space maneuver, inertial hold, and refinements of the analysis performed by the GMI manufacturer and the GPM Inter-calibration Working Group (X-CAL). Tc changes vary from channel to channel and are functions of brightness temperatures. For channels 1-5, the maximum change is around -1.0 K. for other channels, Tc changes are minor.
- Adjusted cold load temperature for 10 GHz channels. This is a minor adjustment and the maximum impact is less than 0.2 K for 10 GHz channels.
- Added a count (earth and cold) adjustment in the magnetism correction equation. This is a minor adjustment and the maximum impact is less than 0.2 K.
- Adjusted magnetic correction coefficients. This is also a minor adjustment and the maximum impact is less than 0.2 K.
- Added Earth-view antenna-induced along-scan corrections. The correction is less than 0.1 K for most pixels along a scan but can be as large as 0.5 K near the edge of scans.

2. For the constellation radiometers, the Level 1C brightness temperature (Tc) data has been intercalibrated to be consistent with the V05 GMI brightness temperature. As a result, V05 AMSR2 Tc decreased 0 to 1.2 K depending on the channel and brightness temperature, ATMS decreased 0 to 0.77 K, MHS decreased 0 to 0.2 K, SSMI/S decreased 0 to 1.05 K, and SAPHIR decreased 0.07 to 0.08 K.

3. Due to sensor issues, SSMI/S F17 37V channel Tc data has been flagged and set to missing during 2016-04-05 to 2016-05-18 (orbits 48595 to 49202) and 2016-08-03 to present (orbits 50286 onward) periods. During these 37V data missing periods, 37H channel Tc was affected and daily means reduced by 2 – 4 K due to lack of cross-pol correction. This issue has been corrected in V05.

4. Noise in the SSMIS F16 91 GHz channels begins to increase significantly in early July of 2015. The noise in the 91V channel starts to get worse in early July and then recovers at the end of August. The 91H channel starts to show issues in July as well, but it doesn't appear to recover until December of 2016. Users should be cautious when using the SSMIS F16 Level 1C data during this period.

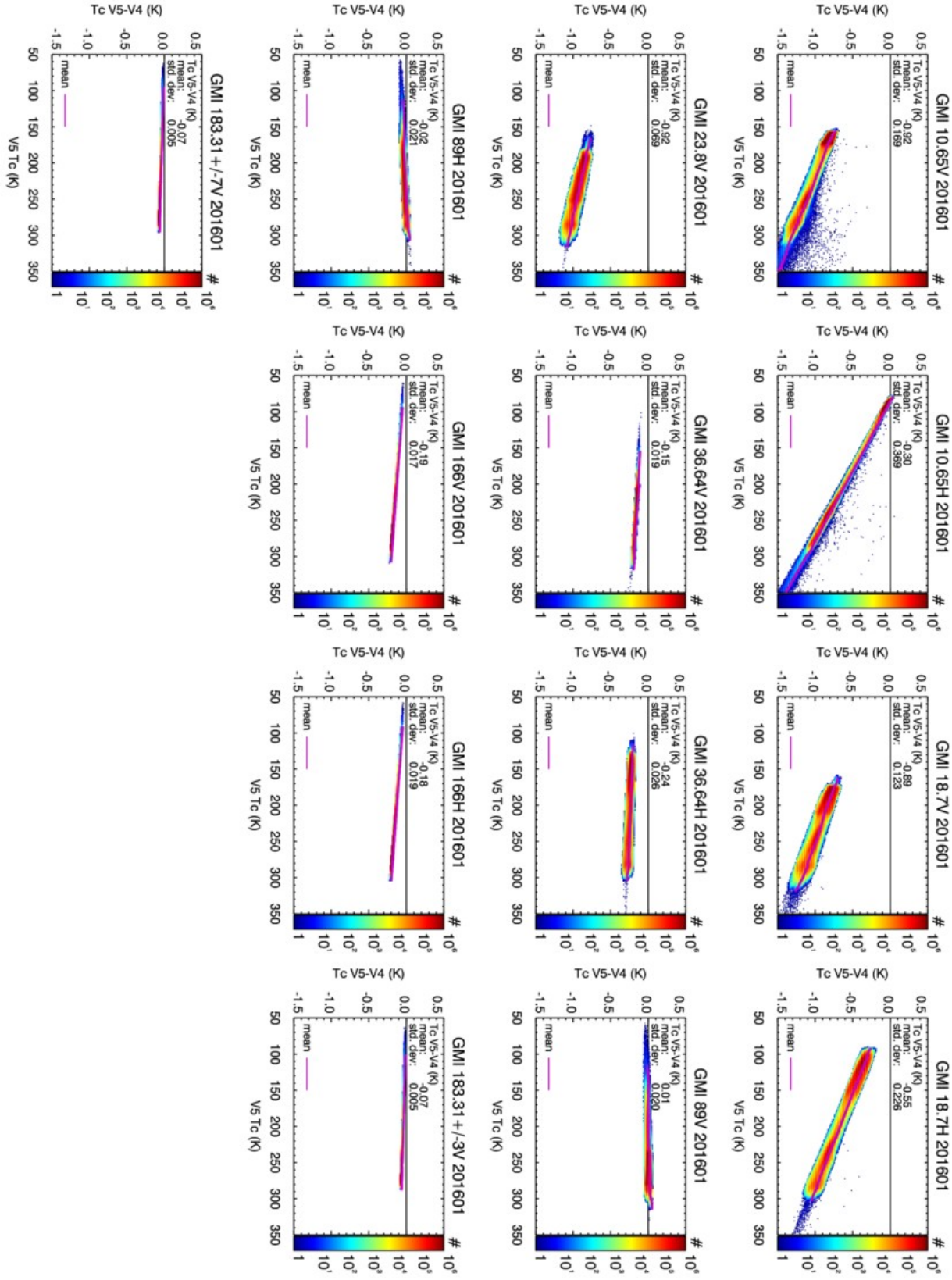

Figure 1: Monthly density plot of L1C GMI Tc difference between V05 and V04.

May 1, 2017

Release Notes for GPROF V05 Public Release

The Goddard Profiling Algorithm is a Bayesian approach that nominally uses the GPM Combined algorithm to create it's a-priori databases. Given the importance of these databases to the final product, they are worth reviewing before discussing particular changes to the algorithm. GPROF V03 was implemented at the launch of the GPM mission and thus had no databases from the GPM satellite itself. Instead, databases were made from a combination of TRMM, Cloudsat, ground based radars and models. V04 used the GPM generated databases but had a very short lead time as the radar and combined algorithm were in flux until nearly the date of the public release. Because the V04 of the Combined algorithm appeared to significantly overestimate precipitation over land, the a-priori databases were constructed from the Combined Algorithm (V04) over ocean, but the DPR Ku (V04) over land and coastal regions. The very short lead time to produce the a-priori databases led to insufficient testing of GPROFV04 that resulted in some less-than ideal retrievals.

GPROF V05 retains the previous version (i.e. V04) of the Combined and DPR-Ku products for its databases. Future versions of GPROF, because of its need for existing GPM products to construct it's a-priori database, will always be one version behind the Combined algorithm. In GPROF V05, we nonetheless improved some of the ice hydrometeor simulations in order to get better agreement between computed and simulated brightness temperatures [ref Sarah]. This leads to smaller bias adjustments in the radiometer simulations and to an overall better fit between the radiometer retrievals and both the Combined products as well as ground validation data.

GPROF V05 made additional changes to retrievals of high latitude oceanic drizzle and snowfall over land. Both of these changes were made because the DPR sensitivity of 12 dBZ was shown to miss substantial amounts of drizzle and light to moderate snowfall events. Because the GPM radars do not have signal in these cases, they are not addressed in the newer versions of the Combined and Radar products either.

Drizzle was addressed in the a-priori database by setting a threshold in the cloud liquid water retrieval from GMI (done before the DPR or Combined rainfall is inserted into the scene), to match the CloudSat based probability of rainfall. This is done for each temperature and Total Precipitable Water (TPW) bin used to subset the a-priori database. While this assumes that higher cloud liquid water amounts correspond to precipitation, the assumption is generally thought to be reasonable. Additional cloud water beyond the CloudSat determined threshold was partitioned between Cloud- and rain water similar to the procedure used by Hilburn and Wentz (2008). This increases rain water at high altitudes to agree better with CloudSat and ERA and MERRA re-analyses but continues to be low relative to these estimates. More work in ongoing to assess high latitude drizzle from different sources.

Over land, the US based MRMS data was used to build a-priori databases for snow covered surfaces of each of the constellations radiometers. Two years of MRMS data were matched up with individual satellite overpasses. This removed much of the low bias that GPROF V04 had over snow covered surfaces.

A final modification made to GPROF V04 is the determination of a precipitation threshold. Whereas GPROF V04 reported an unconditional rain rate and a probability of precipitation, it was up to the user to set a threshold (either in probability or rain rate) if rain/no rain information was needed. While GPROF V05 reports the same information, the algorithm has internally decided if the pixel is precipitating or not, and non-precipitating pixels have been set to zero rainfall. While the original probability of precipitation is still reported, its purpose is only as a diagnostic tool. The user can treat positive rainfall rates as definitively raining. Setting thresholds for precipitation is sometimes difficult in the snowfall where the radiometric information is very limited – particularly for sensors such as AMSR2 that lack high frequency channels. A new quality flag = 2 in therefore introduced.
Quality Flag = 0 still implies that the pixel is good. Quality flag = 1 means there are issues with the retrieval that require caution on the part of the user – particularly for applications such as constructing climate data records. Quality flag = 2 implies the rain/no rain threshold may not be working properly. When the quality flag is set to 3, the retrieved pixel should be used with extreme caution. A complete description of the GPROF quality flag is described below.

Limited validation done by the GPM Validation team shows significantly better correlations and smaller biases with GPROF V05 than GPROF V04. Statistics were run over the Continental United States, Middleton, AK, and over a dense set of rain gauges in the Mountains of Austria. Even more limited validation have been done on snow due to the difficulty in getting reliable ground based measurements. Over the Olympic peninsula (GPM Field Experiment), the total precipitation over the mountains appears correct, but the phase is not. The phase of precipitation in GPROF cannot be determined from the Tb signal itself. Instead, it is determined from the 2 meter temperature and dew point depression (provided by the ancillary data) according to Sims and Liu (2015). Because grid boxes of GANAL or ECMWF are relatively large, they do not capture small-scale terrain variability. Users needing to account for high resolution terrain variability will have to do so as post-processing step in GPROF V05. We hope to correct this in V06.

Almost no validation has been done on the constellation radiometer beyond comparisons of limited coincident overpasses with GMI, and comparisons of monthly means to ensure that the retrieval is performing as expected. AMSR2 comparisons against limited GV observations has similar statistics as GMI for liquid precipitation.

The GPROF output file has a parameter labeled ‘CAPE’. This parameter is set to missing in GPROF V05. It will be use and implemented in subsequent versions.

GPROF 2017 V1 (GPM V5) Quality Flag Description

The GPROF Quality Flag variable for GPM V5 has added one additional index. The old indices in V3 and V4 included values: 0,1,2. The new index can be 0,1,2,3

The description is as follows:

Value 0: pixel is "good" and has the highest confidence of the best retrieval.

Value 1: "use with caution" . Pixels can be set to value 1 for the following reasons:

1) Sunglint is present, RFI, geolocate, warm load or other L1C 'positive value" quality warning flags
2) All sea-ice covered surfaces
3) All snow covered surfaces
4) Sensor channels are missing, but not critical ones.

Value 2: "use pixel with extreme care over snow covered surface" This is a special value for snow covered surfaces only. The pixel is set to 2 if the probability of precipitation is of poor quality or indeterminate. Use these pixels for climatological averaging of precipitation, but not for individual storm scale daily cases.

Value 3: "Use with extreme caution". Pixels are set to value 3 if they have channels missing critical to the retrieval, but the choice has been made to continue the retrieval for these pixels.

Hilburn, K.A. and F.J. Wentz, 2008: Intercalibrated Passive Microwave Rain Products from the Unified Microwave Ocean Retrieval Algorithm (UMORA). *J. Appl. Meteor. Climatol.,* **47**, 778–794, doi: 10.1175/2007JAMC1635.1.

Sims, E.M. and G. Liu, 2015: A Parameterization of the Probability of Snow–Rain Transition. *J. Hydrometeor.,* **16**, 1466–1477, doi: 10.1175/JHM-D-14-0211.1.

Release Notes for the DPR Level 1 products

All users of DPR L1 data should keep in mind the following changes in V5 products.

＜Major changes in the DPR Level 1 products from Version 4 to Version 5＞

1. Changes of the DPR's calibration parameters.
   JAXA improved the DPR's calibration parameters in the Version 5 products based on the new calibration results on orbit. With the new parameters, the measured radar reflectivity factors increase by about +1.3 dB for the KuPR and by about +1.2 dB for the KaPR from the corresponding Version 4 data.

2. Changes of FCIF-LUT.
   The temperature dependence of the FCIF input/output characteristic was improved based on the re-examination of calibration data. The re-examination revealed that the version 4 algorithm compensate the temperature changes too much. In V5, the gain adjustment due to the temperature change is nullified because the actual temperature of FCIF is very stable on orbit.
   The FCIF-LUT for the KuPR near the saturation was improved so that the effect of saturation near the saturation level was mitigated. As for the KaPR, the modification was not made because saturations do not occur in the KaPR in a normal condition.

3. Data format change
   The following two new variables were added and one variable was modified.
   - 'receivedPulseWidth' that indicates the received pulse width after passing through the band-pass-filter was added.
   - 'totalCoefVersion' that indicates the total version, which consists of the version number of the calibration coefficients and the version number of the FCIF-LUT, was added.
   - 'transReceiverCoefVersion' that indicates the version number of the calibration coefficients was modified.

4. Improvement in noise power calculation

The definition of the DPR's noise power was changed. Since the effect of the band-pass filter to noise is different from that of the radar echoes (the former has a continuous flat spectrum while the latter has a non-flat spectrum defined by the transmitting pulse shape), the version 4 algorithm used a formula to calculate the noise power that differs from the formula to calculate the echo power. In version 5, the noise power is also calculated with the formula that is used to calculate the echo powers so that the noise power in V5 is the effective noise power that can be compared with echo powers directly.

＜Caveats for the DPR Level 1 products＞

1. Status of the DPR A-side operation

   JAXA changed that the status of the DPR data obtained during the A-side operation in products Version5 (B-side is used in the current standard operation). The reasons for such handling are that the calibration parameters of the DPR A-side are not reliable, because no external calibration of the DPR A-side was carried out on orbit, and the ground test values of the DPR A-side before launch are not reliable either. Therefore, the corresponding scans were attached with identification flags in the DPR Level 1 products, and these scans were treated as missing scans in the DPR Level 2 products. The following table shows the periods of the DPR A-side nominal operation.

Operational mode	Period	Orbit number
SCDP-B/FCIF-A	2014/3/10~3/12, 5/25	171 - 205, 1351-1355
SCDP-A/FCIF-A	2014/3/14~16	232-262
SCDP-A/FCIF-B	2014/3/16~18	263-295

   B-side (SCDP-B/FCIF-B) is used in the rest of the period.

2. Calculation of the DPR's noise power

   The DPR has a special mode to measure background noise in which the average noise power is measured while the transmitter is turned off at each angle bin in the ordinary observation mode ('Noise-A'). This noise power is subtracted from the received power measured at each range bin to extract radar echo power profile. To calculate the echo profile, the effect of the band-pass filter assumes that the echo has the same power spectrum defined by the transmitted pulse shape. Since the received power is the sum of echo power and noise power, the noise power recorded in each profile is the effective noise ('Noise-B') that affect the echoes. In version 4, Noise-A was calculated by assuming that the noise has a flat spectrum. The difference in the conversion formulas to calculate Noise-A and Noise-B created some confusions to the users although the noise was properly subtracted in the products. In order to avoid the confusion, Noise-A is calculated with the same formula that is used to calculate the echo profile (and hence Noise-B) in version 5. (As a result, the noise power calculated by using the hardware design document is the lower than the power stored in the DPR

L1 product. The magnitudes of difference are -2.11dB, -2.41dB and -2.13dB for the KuPR, the KaPR(MS) and the KaPR(HS), respectively.)

3. Beam directions of the KaPR

JAXA uploaded a proper set of phase code to the KaPR on August 6th, 2014. Until that time from April 8th, 2014, the beam pointing directions of the KaPR had small biases. The code error caused a beam match between the KuPR and the KaPR(MS) and affected the KaPR's total antenna gain slightly. After the proper code was uploaded, the beam scans in the proper directions and the bias error were resolved. The DPR Level 1 algorithm was modified to compensate this bias for the antenna gain in this period so that the antenna gain in the products is correct.

4. Reversal of DPR's scan direction

The beam scan direction of DPR had been reversed from the proper direction until JAXA uploaded a proper set of phase code to the DPR at 13:20 UTC on March 18th, 2014. After the proper code was uploaded, the beam has been scanned in the proper direction, i.e., from left to right with respect to the +X forward direction of the satellite.

The DPR Level 1 algorithm was modified to accommodate this change so that the geolocations in the products are correct from the beginning of the mission.

5. Special operations of DPR

The following caveats describe special operations of DPR. You can use these data with your discretion. You can also refer to the DPR invalid data lists at the following web site. https://www.gportal.jaxa.jp/gp/opeinfo.html

5.1. Operation with the DPR transmitters off

JAXA carried out the receiving only mode to check the DPR receiver system. The orbits in which this operation was performed are shown Appendix-A and operation status in the following

site. https://www.gportal.jaxa.jp/gp/opeinfo.html

5.2. Change of the DPR receiver attenuator (RX ATT) setting

JAXA has checked the dynamic range of the radar system by changing the attenuator setting in the DPR receivers. The received power in the DPR Level 1

products is not affected, because the offset caused by the receiver attenuator is accounted for in the DPR Level 1 algorithm. The orbits in which this operation was performed are shown Appendix-A and operation status in the following site. https://www.gportal.jaxa.jp/gp/opeinfo.html

5.3. Operation of GPM satellite maneuver

NASA has carried out several maneuver operations such as a delta-V maneuver and a Yaw maneuver. In addition, pitch offset maneuvers have also been conducted to check the GPM satellite status. The orbits in which these operations were performed are shown Appendix-A and operation status in the following site. https://www.gportal.jaxa.jp/gp/opeinfo.html

5.4. Test operation for adjusting the phase code in the KuPR instrument

The JAXA DPR project team has conducted several test operations using different phase codes in the phase shifters in order to mitigate the effects of sidelobe clutter in KuPR. Please be cautious of the periods in these test operations. The orbits in which these operations were performed are shown Appendix-A and operation status in the following site. https://www.gportal.jaxa.jp/gp/opeinfo.html

＜Appendix A: Major DPR events＞

Major DPR events until September 2, 2014 are as follows. After September 2, you can visit the following web site to check the DPR status.

https://www.gportal.jaxa.jp/gp/opeinfo.html

Orbit No.	UTC	DPR Event
#144	2014/3/8 21:54	DPR observation start
#171	2014/3/10 16:29	Change DPR FCIF-B to A
#201	2014/3/12 14:24	GPM Delta-V Maneuver
#206	2014/3/12 22:43	DPR power OFF
#207-231	2014/3/13-14	GPM EEPROM change
#232	2014/3/14 14:14	DPR SCDP-A ON
#232	2014/3/14 14:41	DPR check out restart
#236	2014/3/14 20:02	DPR observation restart
#263	2014/3/16 14:08	Change DPR FCIF-A to B
	2014/3/16 14:59	DPR transmitters off (f1/f2 off) test
#264	2014/3/16 15:49	
#279	2014/3/17 15:10	GPM 180deg Yaw Maneuver (+X to -X)
#294	2014/3/18 13:20	Proper phase code upload
#296	2014/3/18 17:18	DPR SCDP-B ON Observation mode
#310	2014/3/19 14:21	GPM Delta-V Maneuver
#325	2014/3/20 13:41	DPR patch adaption
#328	2014/3/20 17:56	DPR observation restart
#374	2014/3/23 17:26	DPR transmitters off observation
#375	2014/3/23 19:05	
	2014/3/23 19:06	SSPA LNA analysis mode
#377	2014/3/23 22:35	DPR observation restart
#380	2014/3/24 2:11	DPR External calibration
#404	2014/3/25 15:07	DPR transmitters off observation
#418	2014/3/26 12:32	
#419	2014/3/26 14:20	GPM Delta-V Maneuver
#478	2014/3/30 9:53	DPR External calibration
#503	2014/4/1 0:00	DPR External calibration (Yaw + pitch)
#531	2014/4/2 19:47	GPM Delta-V Maneuver
#601	2014/4/7 7:37	DPR External calibration

Orbit No.	UTC	DPR Event
#621	2014/4/8 14:10	Upload new test phase code of KuPR (#1)
#626	2014/4/8 21:46	DPR External calibration (Yaw + pitch)
#647	2014/4/10 6:36	DPR External calibration
#672	2014/4/11 20:43	DPR External calibration (Yaw + pitch)
#675	2014/4/12 1:45	GPM Delta-V Maneuver
#715	2014/4/14 15:28	Upload new test phase code of KuPR (#2)
#731	2014/4/15 15:44	Return to phase code (#1)
#675	2014/4/12 1:45	GPM Delta-V Maneuver
#747	2014/4/16 17:04	GPM Delta-V Maneuver
#748	2014/4/16 17:39	DPR transmitters off observation
#763	2014/4/17 17:07	
#770	2014/4/18 4:22	DPR External calibration (Yaw + pitch)
#795	2014/4/19 18:31	DPR External calibration (Yaw + pitch)
#795	2014/4/19 18:55	Ku/Ka RX ATT change 6dB to 9dB
#810	2014/4/20 17:59	Ku/Ka RX ATT change 9dB to 12dB
#824	2014/4/21 15:36	Ku/Ka RX ATT change 12dB to 6dB
#827	2014/4/21 20:34	GPM Delta-V Maneuver
#885	2014/4/25 13:05	GPM ST alignment and IRUCAL table updates
#886	2014/4/25 14:30	GPM +10 deg. roll slew
	2014/4/25 15:20	GPM +10 deg. pitch slew
#887	2014/4/25 16:10	GPM +10 deg. yaw slew
#901	2014/4/26 13:30	GPM 180deg Yaw Maneuver (-X to +X)
#907	2014/4/27 0:00	GPM -1 deg. pitch slew
#913	2014/4/27 8:20	GPM -1 deg. pitch slew (-2 deg. total)
#918	2014/4/27 16:20	GPM -2 deg. pitch slew (-4 deg. total)
#923	2014/4/28 0:25	
#924	2014/4/28 1:10	Ku/Ka RX ATT change 6dB to 9dB
#933	2014/4/28 15:04	Upload new test phase code of KuPR(#3)
#935	2014/4/28 18:13	Return to phase code(#1)
#964	2014/4/30 15:50	GPM Delta-V Maneuver
#994	2014/5/2 13:20	Upload new test phase code of KuPR (#4)
	2014/5/2 13:21	Ku/Ka RX ATT change 9dB to 6dB
#996	2014/5/2 16:36	Upload new test phase code of KuPR(#5)
#998	2014/5/2 19:44	Ku/Ka RX ATT change 6dB to 9dB

Orbit No.	UTC	DPR Event
	2014/5/2 19:45	Return to phase code (#1)
#1059	2014/5/6 17:35	GPS both A and B ON
#1103	2014/5/14 13:44	
#1073	2014/5/7 15:57	GPM Delta-V Maneuver
#1088	2014/5/8 14:15	Ku SSPA analysis mode (5min)
	2014/5/8 15:08	Ka SSPA analysis mode (5min)
#1089	2014/5/8 15:48	Ku LNA analysis mode (5min)
	2014/5/8 16:44	Ka LNA analysis mode (5min)
#1090	2014/5/8 17:23	Upload new test phase code of KuPR (#6)
#1092	2014/5/8 20:21	Ka SSPA analysis mode (5min)
	2014/5/8 21:12	Upload new test phase code of KuPR (#7)
#1094	2014/5/9 0:16	Return to phase code(#1)
#1150	2014/5/12 14:58	Ku/Ka RX ATT change 9dB to 12dB
#1182	2014/5/14 16:07	GPM Delta-V Maneuver
#1274	2014/5/20 13:30	GMI Deep Space Calibration
#1277	2014/5/20 18:44	
#1288	2014/5/21 11:30	Upload new test phase code of KuPR (#8)
#1290	2014/5/21 14:43	Upload new test phase code of KuPR (#9)
#1292	2014/5/21 17:59	Upload new test phase code of KuPR (#10)
#1294	2014/5/21 21:07	Upload new test phase code of KuPR (#11)
#1296	2014/5/22 0:16	Return to phase code(#1)
#1319	2014/5/23 11:38	Upload new test phase code of KuPR (#12)
#1322	2014/5/23 15:03	Upload new test phase code of KuPR (#13)
#1324	2014/5/23 15:03	Upload new test phase code of KuPR (#14)
#1326	2014/5/23 21:37	Upload new test phase code of KuPR (#15)
#1328	2014/5/24 0:57	Return to phase code(#1)
#1351	2014/5/25 11:44	Change DPR FCIF-B to A (For External Cal.)
		Ku/Ka RX ATT change 12dB to 6dB
#1354	2014/5/25 17:18	DPR External calibration (Yaw + pitch)
#1355	2014/5/25 17:54	Change DPR FCIF-A to B
		Ku/Ka RX ATT change 6dB to 12dB
#1414	2014/5/29 13:59	GPM Delta-V Maneuver
#1430	2014/5/30 13:50	Upload new test phase code of KuPR (#16)
#1431	2014/5/30 15:26	Upload new test phase code of KuPR (#17)

Orbit No.	UTC	DPR Event
#1432	2014/5/30 17:01	Upload new test phase code of KuPR (#18)
#1433	2014/5/30 18:34	Upload new test phase code of KuPR (#19)
#1434	2014/5/30 20:07	Return to phase code(#1)
#1447	2014/5/31 16:06	Upload new test phase code of KuPR (#20)
#1448	2014/5/31 17:53	Upload new test phase code of KuPR (#21)
#1449	2014/5/31 19:59	Return to phase code(#1)
#1477	2014/6/2 15:06	DPR External calibration
#1502	2014/6/4 5:15	DPR External calibration
#1508	2014/6/4 14:13	Upload new test phase code of KuPR (#22)
#1508	2014/6/4 14:56	Upload new test phase code of KuPR (#23)
#1509	2014/6/4 16:39	Upload new test phase code of KuPR (#22)
#1511	2014/6/4 18:59	Return to phase code(#1)
#1539	2014/6/6 14:09	Upload new test phase code of KuPR (#22)
#1541	2014/6/6 17:26	Return to phase code(#1)
#1600	2014/6/4 5:15	DPR External calibration
#1603	2014/6/10 17:38	GPM 180deg Yaw Maneuver (+X to -X)
#1625	2014/6/12 2:58	DPR External calibration
#1646	2014/6/13 11:46	DPR External calibration
#1648	2014/6/13 14:08	Upload new test phase code of KuPR (#24)
#1649	2014/6/13 15:45	Upload new test phase code of KuPR (#25)
#1650	2014/6/13 17:36	Upload new test phase code of KuPR (#26)
#1651	2014/6/13 19:12	Upload new test phase code of KuPR (#27)
#1652	2014/6/13 20:54	Upload new test phase code of KuPR (#28)
#1653	2014/6/13 22:33	Upload new test phase code of KuPR (#29)
#1654	2014/6/14 0:21	Upload new test phase code of KuPR (#30)
#1655	2014/6/14 1:39	Return to phase code(#1)
#1726	2014/6/18 15:17	GPM Delta-V Maneuver
#1769	2014/6/21 9:33	DPR External calibration
#1794	2014/6/22 23:42	DPR External calibration (Yaw + pitch)
#1892	2014/6/29 7:18	DPR External calibration
#1917	2014/6/30 21:27	DPR External calibration
#1942	2014/7/2 12:42	Upload new test phase code of KuPR (#31)
#1944	2014/7/2 14:38	Upload new test phase code of KuPR (#32)
#1945	2014/7/2 16:30	Return to phase code(#1)

Orbit No.	UTC	DPR Event
#1975	2014/7/4 15:07	Upload new test phase code of KuPR (#33)
#1976	2014/7/4 16:44	Upload new test phase code of KuPR (#34)
#1977	2014/7/4 18:24	Return to phase code(#1)
#2015	2014/7/7 5:01	DPR External calibration
#2040	2014/7/8 19:08	DPR External calibration (Yaw + pitch)
#2053	2014/7/9 16:17	GPM Delta-V Maneuver
#2163	2014/7/16 16:32	GPM 180deg Yaw Maneuver (-X to +X)
#2176	2014/7/17 13:22	Upload new test phase code of KuPR (#35)
#2177	2014/7/17 15:03	Upload new test phase code of KuPR (#36)
#2178	2014/7/17 16:37	Upload new test phase code of KuPR (#37)
#2180	2014/7/17 18:47	Return to phase code(#1)
#2184	2014/7/18 1:42	DPR External calibration
#2209	2014/7/19 15:51	DPR External calibration
#2286	2014/7/24 14:54	Change Ku timing delay
#2289	2014/7/24 19:11	Upload new test phase code of KuPR (#38)
#2290	2014/7/24 20:49	Return to phase code(#1)
#2304	2014/7/25 18:07	Upload new test phase code of KuPR (#39)
#2307	2014/7/25 23:26	DPR External calibration
#2332	2014/7/27 13:34	DPR External calibration
#2380	2014/7/30 16:04	GPM Delta-V Maneuver
#2430	2014/8/2 21:12	DPR External calibration (Yaw + pitch)
#2455	2014/8/4 11:21	DPR External calibration
#2455	2014/8/6 20:48	Upload new phase code of KaPR
#2599	2014/8/13 17:55	DPR External calibration
#2624	2014/8/15 8:03	DPR External calibration
#2706	2014/8/20 15:09	GPM Delta-V Maneuver
#2722	2014/8/21 15:40	DPR External calibration
#2747	2014/8/23 5:48	DPR External calibration
#2782	2014/8/25 12:15	Change DPR FCIF-B to A
#2782	2014/8/25 12:30	Upload new test phase code of KuPR (FCIF-A#1)
#2784	2014/8/25 14:34	Upload new test phase code of KuPR (FCIF-A#2)
#2785	2014/8/25 16:13	Upload new test phase code of KuPR

Orbit No.	UTC	DPR Event
		(FCIF-A#3)
#2786	2014/8/25 17:51	Upload new test phase code of KuPR (FCIF-A#4)
#2787	2014/8/25 19:22	Change DPR FCIF-A to B
#2787	2014/8/25 19:24	Return to phase code(#39)

Release Notes for the DPR V5 Level 2 products

All users of DPR L2 data should keep in mind the following changes in V5 products.

This document describes only the major changes in the level 2 products. There are some changes in level 1 that affect the level 2 products. Please refer to "Release Notes for the DPR Level 1 products" for the details of the changes in level 1 products.

Among several changes in level 1 products, the important changes that affect level 2 products substantially are the following points.
The DPR's system parameters were re-examined. Based on the new calibration results, the offset parameters for the transmitting powers, receiver's gains, the beam widths, and the pulse width of both KuPR and KaPR are redefined. As a result, Zm of KuPR has increased by about +1.3 dB, and Zm of KaPR by about +1.2 dB. The radar surface cross section (sigma0) of KuPR has increased by about +1.2 dB and that of KaPR by about +1.1 dB, although the changes in sigma0 depend slightly on the incidence angle due to the changes in the beam widths. Because of the introduction of the adjustment factors in L2 (see below) whose magnitudes vary with time, the numbers mentioned above are not fixed numbers but change with time, especially near the beginning of the GPM mission. In fact, for example, statistics show that an average (over angle) increase in sigma0 at Ku-band is about +1.0 dB, that at Ka(MS) is about +0.6 dB and that at Ka(HS) is about +0.9 dB on the first 5 days in June 2014.

- The FCIF-LUT for the KuPR near the saturation was improved so that the effect of saturation near the saturation level was mitigated.

Changes in level 2 algorithm

- In addition to the changes in the DPR L1 calibration, adjustment factors are introduced to remove small trends in the overall system gains in KuPR and KaPR. The adjustment factors change the measured received powers only by a small fraction of dB.
- Since the FCIF-LUT for the KuPR near the saturation level was modified to mitigate the effect of saturation, the statistics of sigma0 near the saturation

level in the KuPR has changed. This change affects the SRT performance as well. The side-lobe echo cancellation parameters are adjusted to cope with this change as well

- Measured radar reflectivity factor Zm and surface radar cross section sigma0 are calculated based on the new values of the pulse widths of both KuPR and KaPR. Accordingly, the angle bin dependence of sigma0 has changed slightly.
- A DSD database that depends on the month, region, surface type and rain type was created from the statistics of DSD parameters estimated with the dual-frequency algorithm. The R-Dm relationship in the DSD database is used as the default R-Dm relationship in the single frequency (Ku-only and Ka-only) data processing before it is modified by other constraints such as the path-integrated attenuation. The introduction of the DSD database has modified the precipitation estimates substantially when they are light (less than about 3mm/h) in many cases. Rain estimates from the Ku-only and dual-frequency algorithms now agree very well.
- New flags are introduced. They are `snowIceCover` in the preparation module, `flagHeavyIcePrecip` and `flagAnvil` in the classification module, and `flagSurfaceSnowfall` and `surfaceSnowfallIndex` in the experimental module. The meanings of these flags should be referred to the user's manual.
- Winter convective storms that give large DFRm (measured Dual-Frequency Ratio) at the storm top are flagged and the corresponding pixels are classified as convective in V5. This category only appears in the inner swath since DFRm is available only there.

Release Notes for GPM SLH V5

July 11, 2017

In GPM SLH V5, LUT for mid and higher latitudes is newly developed. LUT for tropics is the same as TRMM SLH V7A except for using GPM/KuPR information instead of TRMM/PR information as inputs. Some recommendations to users of orbital data are listed below, for SLH V5 retrieved as tropical precipitation or those as mid latitude precipitation. The separation between the tropics and the mid latitudes should be done referring to the rainTypeSLH values stored in the orbital data, and described in Table 1.

Table 1. description for rainTypeSLH

(a) Tropics and subtropics	(b) Mid and higher latitudes
0: No precipitation 1: Convective 2: Shallow stratiform 3: Deep stratiform 4: Deep stratiform with low melting level 5: Intermediary 6: Other	0: No precipitation 110: Convective 121: Shallow stratiform 122: Deep stratiform, downward decreasing 123: Deep stratiform, downward increasing 124: Deep stratiform, subzero 160: Other
Mask	
900: Tibet, winter mid-lat etc. 910: Suspicious extreme	

(i) No precipitation or Masked out pixels (rainTypeSLH=0, 900, or 910)

SLH values are not estimated.

(ii) Caveats for tropical algorithm (0< rainTypeSLH <10)

Analysis showed consistency among GPM SLH V4, V5 and TRMM SLH V7A estimates over the coverage of TRMM/PR during a GPM and TRMM overlapping observation period (April-June 2014). Note that:

0. Vertical levels are changed from 19 levels to 80 levels.
1. Shallow non-isolated echo has been classified as stratiform by rain type

classification algorithm for TRMM/PR, but as convective by that for GPM/KuPR, affecting SLH estimates. To give consistent SLH estimates from GPM/KuPR with those from TRMM/PR, shallow non-isolated echo is classified as stratiform in GPM SLH V4.

2. Differences of sampling between TRMM/PR and GPM/KuPR affect SLH estimates. The greater global coverage of the GPM Core Observatory (65°N/S) compared to the TRMM coverage (35°N/S) decreases sampling of GPM/DPR over the coverage of TRMM/PR, especially at around the satellite inclination latitudes of 35°N/S, affecting SLH estimates there.
3. Retrieval for high mountains/winter mid-latitudes pixels will be developed.
4. For tropical latent heating, due to the change of vertical levels from 19 levels to 80 levels, users are recommended to smooth the profile vertical for a few levels to avoid the spurious peak at around 0degC level.

(iii) Caveats for Mid-latitude algorithm (rainTypeSLH>100)

A. In look up table ranges where sampling numbers did not satisfy the criteria, values are discarded or extrapolated from nearest neighbor bins, depending on the precipitation type. Sampling number criterion is basically 30, but 60 is chosen for deep stratiform LUT with precipitation maximum at the near surface level. Corresponding range for the convective LUT is PTH>10.5km.

B. Recommendation for horizontal averaging at the utilization of products 2HSLH or 3GSLH of GPM SLH V05.

B1. Eddy flux convergence in Q1R and Q2 are estimated assuming that the size of "large-scale grids" is 100kmx100km. Therefore, it is recommended to average horizontally in this spatial scale to utilize Q1R or Q2.

B2. Horizontal averaging of about 50km x 50km, or 100 pixels with GPM DPR sampling, is recommended, in order to limit root mean square errors (RMSE) calculated between estimated LH from LFM-simulated precipitation, less than a half of the mean value at the LH peak height of ~5.5km (for Case 1).

October 4, 2017

Release note for GPM Global Rainfall Map (GPM-GSMaP)

The GPM Global Rainfall Map (GPM-GSMaP) Level 3 product version 04A (Algorithm version 7) was released to the public since January 17, 2017, V04B was released since Mach 2, 2017, V04C was released since Mach 27, 2017, and V04D was released since May 9, 2017. However, because of program issues, the GPM-GSMaP Level 3 product version 04E was released to the public since October 4, 2017.

Updates from version 04D to version 04E

- Improvement in handling abnormal IR values in the GSMaP_MVK algorithm
- Fix of a very minor issue of the GSMaP_GMI algorithm

Updates from version 04C to version 04D

- Install of a table related to the Tb calibration of GMI L1 V05

Updates from version 04B to version 04C, connected with bug-fixing of "PrecipRateGC" in the following products.

- All standard products in V04A
- Standard products since March 1, 2017 in V04B.

Updates from version 04A to version 04B are following.

- Adding a missing value in "snowProbability" of the GSMaP Hourly (3GSMAPH).
- Bug-fixing in "snowProbability" of the GSMaP Monthly (3GSMAPM).
- Bug-fixing in "satelliteInfoFlag".

Update from version 03 (Algorithm version 6) to version 04A (Algorithm version 7) are following.

1) Improvement of the GSMaP algorithm using GPM/DPR observations as its database
2) Implementation of a snowfall estimation method in the GMI & SSMIS data and a screening method using NOAA multisensor snow/ice cover maps in all sensors
3) Improvement of the gauge-correction method in both near-real-time and standard products
4) Improvement of the orographic rain correction method
5) Improvement of a weak rain detection method over the ocean by considering cloud liquid water

For details, following URLs can be helpful for your reference.
http://www.eorc.jaxa.jp/GPM/doc/product_info/release_note_gsmapv04-v7_en.pdf

(For the Japanese)

http://www.eorc.jaxa.jp/GPM/doc/product_info/release_note_gsmapv04-v7_ja.pdf

Followings are remarks and known bugs in current version of GPM-GSMaP product to be fixed in future versions.

Remaining problems

A. Retrieval issues

1. The snowfall estimation method for the GMI & SSMIS data was installed in the V04 product, but it still needs to be validated and improved further. In addition, several biases and/or gaps may be appeared in the mid-latitude ocean, due to changes of the estimation method. In addition, sometimes, surface snow or sea ice may be misidentified as precipitation signal, especially in spring season. Users should be cautious of estimations over the cold surface (in particular, below 273.2 K).
2. The orographic/non-orographic rainfall classification scheme has been implemented in the GSMaP algorithm for passive microwave radiometers (Yamamoto and Shige, 2014). The scheme is switched off for regions (e.g. the Sierra Madre Mountains in the United States and Mexico) where strong lightning activity occurs in the rainfall type database because deep convective systems for the regions are detected from the scheme involved in the orographic rain condition. The scheme improves rainfall estimation over the entire Asian region, particularly over the Asian region dominating shallow orographic rainfall. However, overestimation and false-positive of orographic rainfall remain. This is because the orographic rainfall conditions have moderate thresholds for global application. We examine to resolve their problems.
3. The precipitation estimation of gauge-calibrated hourly rainfall product (GSMaP_Gauge) depends on a large part on the Climate Prediction Center (CPC) Unified Gauge-Based Analysis of Global Daily Precipitation data sets provided by NOAA. If the CPC data sets have good estimation of precipitation in a region, the GSMaP_Gauge data sets also will show good scores in the region. However, in case the CPC data sets under or overestimate the rain fall rate seriously or miss the rainfall event, the GSMaP_Gauge product also estimates or misses the precipitation in a similar manner as the CPC data sets. Note that the CPC data sets and hence the GSMaP_Gauge data do not always show accurate estimation particularly over less dense gauge region.
4. Although the GSMaP_Gauge_NRT is a near real time version of the GSMaP_Gauge, the products does not use the gauge measurement directly. Since the global gauge measurement takes much time to collect and process the data from all over the world, the gauge data is not available in near real time. Hence, in the GSMaP_Gauge_NRT product, only the error parameters derived from the GSMaP_Gauge are used to adjust the GSMaP_NRT estimation, which is named as the GSMaP_Gague_NRT. We would like to know evaluation and validation results of this product for improvement. We appreciate if you give us some feedback.

B. Calibration issues

5. Brightness temperatures used in rainfall retrievals of GCOM-W/AMSR2 and GPM-Core/GMI are bias-corrected using parameters provided by JAXA. These parameters may be modified in future when calibration of each Level 1B data is updated.

6. Scan errors may be occasionally found in rainfall retrievals of SSMIS (microwave imager/sounder) on board the DMSP-F16, DMSP-F17 and DMSP-F18 satellites. This problem will be corrected in the future version of L1c data.
7. MHS data used in the GSMaP product was changed form Level 1B to Level 1C. The Scattering Index (SI) in the AMSU-A/MHS algorithm is changed at altitude higher than 40 degrees. However, we have not yet fully evaluated the effect. We would like to know evaluation and validation results of the GSMaP AMSU-A/MHS rainfall retrievals. We appreciate if you give us some feedback.

March 20, 2017

Caveats for the CMB Level 2 Product in the GPM V05 Public Release

The Combined Radar-Radiometer Algorithm (CMB) L2 V05 product includes precipitation estimates over the broader, NS (Ku+GMI) swath as well as estimates over the narrower, MS (Ku+Ka+GMI) swath. The input of the CMB L2 algorithm is derived from DPR L2 and GMI L1 products. In particular, the CMB L2 algorithm depends upon inputs from the DPR L2 Preparation Module, Classification Module, Surface Reference Technique Module, and the Vertical Structure Module. From GMI L1, the CMB L2 algorithm utilizes the intercalibrated brightness temperature observations.

During the early GPM mission (prior to June 2014) many tests and modifications of the DPR performance were carried out, and these had an impact on not only DPR products but also the CMB L2 estimates that depend on them. Therefore, CMB L2 precipitation estimates from the early mission should be used with caution. A listing of the orbits impacted by these tests and modifications can be obtained from the GPM Radar Team.

Mainlobe and sidelobe clutter contamination of DPR reflectivities is reduced using radar beam reshaping and statistical corrections. The combination of these applications reduces clutter successfully over most surfaces, but there are still "exceptional" regions where clutter signatures are still evident. Also, ice-covered land surfaces produce Ku-band radar surface cross-sections at nadir view that sometime exceed the upper limit of the radar receiver range. Estimates of Ku-band path-integrated attenuation from the Surface Reference Technique Module are possibly biased in these regions. Since radar reflectivities and path-integrated attenuations are utilized by the CMB L2 algorithm, precipitation estimates in these "exceptional" regions should be used with caution.

The current CMB L2 algorithm uses the Ku-band radar reflectivities from the Preparation Module to detect either liquid- or ice-phase precipitation. The lowest detectable reflectivity for DPR at Ku band is ~13 dBZ, and so light snow or very light rainfall may not be detected and quantified by the algorithm.

In addition to the impact of input data from DPR L2, there are uncertainties due to the current limitations of the CMB L2 algorithm's physical models and other assumptions that also have an impact on precipitation estimates. In particular, the physical models for scattering by ice-phase precipitation particles now feature realistic nonspherical particle geometries but are still undergoing development. The scattering models for ice- and mixed-phase precipitation will likely be improved in future product releases. Also, the effects of radar footprint non-uniform beamfilling and multiple scattering of transmitted power are addressed in CMB L2, but the

mitigating strategies are not yet generalized and have not been analyzed in detail. Multiple scattering primarily affects Ka-band reflectivities, and sometimes eliminates earth surface reflection in regions of strong radar attenuation, while footprint non-uniform beamfilling impacts the interpretation of both Ku- and Ka-band radar data. As a consequence, both NS and MS mode precipitation estimates associated with intense convection, in particular, should be treated with caution. Finally, the assumed *a priori* statistics of precipitation particle size distributions can have an influence on estimated precipitation. As particle size distribution data are collected during the mission, more appropriate assumptions regarding the *a priori* statistics of particle sizes will be specified in the algorithm. At this stage of the mission, however, relatively simple assumptions regarding particle size distributions have been introduced into the algorithm, and so biases in estimated precipitation and underlying particle size distributions can occur.

It should also be noted that both precipitation estimates and retrievals of environmental parameters from CMB L2 have not yet been comprehensively validated using ground observations. Such a validation effort is under way and will continue after the V05 release of the CMB L2 product. Therefore, it is very important that users of the public release product keep in contact with the CMB Team for updates on the validation of precipitation estimates and any reprocessing's of the CMB L2 algorithm product.

Preliminary validation of the CMB L2 V05 product has revealed good consistency between estimated surface precipitation rate and raingage-calibrated radar, with correlations ~ 0.85 between 0.5 degree-resolution instantaneous estimates of surface precipitation rate and gage-calibrated radar (Multi-Radar Multi-Sensor [MRMS] product) over the continental US and coastal waters. Overall, there is a low bias of NS and MS mode rain rates on the order of a few percent. Zonal mean precipitation rates agree well with zonal mean precipitation rates from the Global Precipitation Climatology Project (GPCP) product within the 40 ^{o}S to 40 ^{o}N latitude band. Estimated zonal means at higher latitudes are underestimated relative to GPCP, due in part to the limited sensitivity of the DPR radar to light snow and drizzle. In the global mean, NS and MS mode estimates differ by less than a percent. Although there is good agreement and consistency of large-scale mean precipitation estimates between 40 ^{o}S and 40 ^{o}N, regional and seasonal means exhibit biases that are the subject of current investigations.

There could potentially be significant changes in the CMB L2 rain rate products in the transition from V05 to V06 due to possible tuning of the DPR radar calibration as well as adjustments and improvements of the CMB algorithm. Again, the users of the V05 public release product should keep in contact with the CMB Team for information regarding these changes.

CMB L2 V04 to V05 Changes

Numerous modifications have been made to the CMB L2 algorithm in the transition from V04 to V05, and the significant updates are summarized here. It may be noted at the outset, however, that the basic algorithm mechanics (i.e., estimation methodology) has not changed. The estimation method filters ensembles of DPR Ku reflectivity-consistent precipitation profiles using the DPR Ka reflectivities, path integrated attenuations and attenuated surface radar cross-sections at Ku and Ka bands, and GMI radiances. The filtered profile ensembles are consistent with all of the observations and their uncertainties, and the mean of the filtered ensemble gives the best estimate of the precipitation profile. The output file structure is essentially the same as in CMB V04, but a few additional variables are included for diagnostic purposes.

In the CMB V03 and V04 algorithms, estimated precipitation profiles were constrained by estimates of total path-integrated attenuation from the satellite to the earth's surface, derived from the DPR algorithm's surface reference technique (SRT) module; Grecu et al. (2016). However, an alternative approach is to develop a model for the normalized radar cross-section (σ^0) of the surface at the Ku and Ka channel frequencies of the DPR and relate that to a model of the surface emissivities (ε) at the GMI frequencies. Such a σ^0/ε model was developed by Munchak et al. (2016). The model is used to effectively constrain the simulated surface σ^0/ε in the algorithm's simulations of attenuated surface cross-section and upwelling brightness temperatures, which are compared to the observed attenuated cross-sections and brightness temperatures. In the CMB V05 algorithm, both the path-integrated attenuations and attenuated surface cross-sections are utilized to constrain solutions, even though there is some redundancy between these two observables. It should be noted, however, that some redundancy in the information content of observations leads to greater suppression of uncorrelated noise in algorithm estimates.

Another new feature of the V05 algorithm involves the algorithm's simulation of path-integrated attenuation at Ka band. Using off-line, high-resolution simulations of attenuation based upon ground-based radar fields, it was determined that the Ka-band path-integrated attenuation in vertical columns over DPR-sized footprints, derived using a Hitschfeld-Bordan method as it is done in the CMB algorithm, is significantly overestimated in convective regions where the footprints are partially filled with precipitation. The degree of partial filling, however, can be estimated using a 3x3 array of DPR footprints centered on the footprint of interest. In the CMB V05 algorithm, a scaling parameter based on the 3x3 array is used to modify the Hitschfeld-Bordan derived path-integrated attenuation at Ka band to properly account for partial filling of the radar footprint by precipitation. At Ku band, the effects of partial footprint filling on path-integrated attenuation are much smaller and are neglected in CMB V05.

The CMB V04 algorithm estimates exhibited a lack of sensitivity to path-integrated attenuation, such that the scaling of estimated attenuation relative to reflectivity was sometimes inappropriately high (i.e., the scaling was adjusted little from the initial guess), leading to overestimation of rain rates. Two changes are introduced into the CMB V05 algorithm to obtain more appropriate sensitivity. First, the prescribed uncertainties of SRT-derived path-integrated attenuations are reduced, forcing greater fidelity of solutions to observed path-integrated attenuations. Second, weak empirical constraints between particle size distribution mass-weighted mean diameters (D_m) and normalized intercepts (N_w) are imposed, such that larger D_m values tend to correlate with lower N_w values. The impact is a tendency for heavier rains not to amplify attenuation relative to reflectivity as much as before. The two changes described here lead to lower rain rates, particularly in moderate to heavy precipitation regions over land, using CMB V05.

Another aspect of the algorithm that is improved in V05 is the description of scattering by ice-phase precipitation particles. In all versions through V04, ice-phase precipitation particles were represented as spherically shaped, homogeneous mixtures of ice and air. In CMB V05, ice-phase precipitation in stratiform regions is represented using nonspherical particles with realistic geometries, as described in Kuo et al. (2016) and Olson et al. (2016). The rigorously computed microwave single-scattering properties of these particles are included in the algorithm's scattering tables. The nonspherical ice particles are less strongly forward scattering than spherical particles of the same mass, leading to substantially lower simulated upwelling microwave radiances at the higher-frequency GMI channels. The impact is to reduce CMB V05 algorithm-estimated snow water contents, since less snow is required to produce the same signal at the higher frequency channels. Mixed-phase particles are still described using spherical geometry models in V05.

The prescribed uncertainty of any observation in the CMB algorithm represents both the noise in the observation as well as the error in the simulation of that observation by the algorithm's forward model, and therefore it determines the degree to which the observation impacts estimates produced by the ensemble filter. As previously mentioned, the prescribed uncertainties of Ka-band reflectivities and Ku- and Ka-band path-integrated attenuations are modified in CMB V05. In addition, attenuated σ^0 observations are also introduced, and these observations are assigned uncertainties based on the variances of σ^0 for the given earth surface type, incidence angle, and wind conditions based upon a climatology of σ^0; see Munchak et al. (2016).

The prescribed uncertainties of Ka-band reflectivities are reduced from 3 dB in V04 to 2 dB in CMB V05. The uncertainty of Ku-band path-integrated attenuations is reduced from 4 dB to 3 dB. If path-integrated attenuation at Ka-band is available, the difference of the path-integrated attenuations (Ka – Ku) is used as an observable, with a prescribed uncertainty reduced from 4 dB to 2 dB in V05. This reduction of uncertainty is in recognition of the fact that the Ka-Ku path-integrated attenuation

difference in non-precipitation situations provides a more stable reference relative to that of either one of the two channels. Over open water surfaces, the uncertainties of the σ^0 at Ku and Ka band are set to the climatological variabilities of σ^0 in those bands, given the 10-m wind speed derived from reanalysis data. For other surfaces, the uncertainty of Ku σ^0 is also derived from its climatological variability, but it is limited to values above 2 dB, while the uncertainty of the Ka σ^0 is limited to values above 4 dB. Uncertainties in brightness temperatures are maintained at the V04 values of 5 K (at or below 37 GHz) and 6.1 K (above 37 GHz).

Grecu, M., W. S. Olson, S. J. Munchak, S. Ringerud, L. Liao, Z. S. Haddad, B. L. Kelley, and S. F. McLaughlin, 2016: The GPM Combined Algorithm. *J. Atmos. and Oceanic Tech.*, **33**, 2225-2245.

Kuo, K.-S., W. S. Olson, B. T. Johnson, M. Grecu, L. Tian, T. L. Clune, B. H. van Aartsen, A. J. Heymsfield, L. Liao, and R. Meneghini, 2016: The microwave radiative properties of falling snow derived from nonspherical ice particle models. Part I: An extensive database of simulated pristine crystals and aggregate particles, and their scattering properties. *J. Appl. Meteor. and Climatol.*, **55**, 691-708.

Munchak, S. J., R. Meneghini, M. Grecu, and W. S. Olson, 2016: A coupled emissivity and surface backscatter cross-section model for radar-radiometer retrieval of precipitation over water surfaces. *J. Atmos. Oceanic Technol.*, **33**, 215-229.

Olson, W. S., L. Tian, M. Grecu, K.-S. Kuo, B. T. Johnson, A. J. Heymsfield, A. Bansemer, G. M. Heymsfield, J. R. Wang, and R. Meneghini, 2016: The microwave radiative properties of falling snow derived from nonspherical ice particle models. Part II: Initial testing using radar, radiometer and in situ observations. *J. Appl. Meteor. Climatol.*, **55**, 709 – 722.

Release Notes for the CSH V05 Level 3 gridded product (3GCSH)

5 July 2017

Changes from V04:

Major changes from V04 include the retrieval of latent heating (LH) over the entire GPM domain (i.e., 67N to 67S), not just the TRMM domain (i.e., 37N to 37S). However, the other remaining CSH products (i.e., eddy heating, microphysical and eddy moistening, and radiation) are still retrieved only over the TRMM domain.

All products are now retrieved at 80 vertical levels every 250 meters AGL starting at the surface (i.e., 0, 250, 500, etc.).

The retrievals for the Tropics (i.e., TRMM domain) are based upon an updated version of the previous CSH algorithm design (Tao et al. 2010). The algorithm still relies upon look-up-tables (LUTs) of model-simulated heating/moistening profiles generated from the Goddard Cumulus Ensemble Model (or GCE), a CRM, which are stored and mapped to satellite grids according to precipitation characteristics. In V04, the previous TRMM V7 CSH LUTs were used. Those LUTs were designed for 0.5 x 0.5 degree TRMM grids (versus the 0.25 x 0.25 degree GPM grids), so the GPM input data in V04 were pre-smoothed to accommodate the coarser resolution of the LUTs. In V05, the LUTs are generated at the GPM grid resolution (0.25 degrees) and are based on 2D multi-week simulations for 6 ocean (vs 5) and 4 land (vs 2) cases (**see Table 1**) using larger domains (512 vs 256 km) and an improved Goddard 4ICE (Lang et al. 2014; Tao et al. 2016) microphysics scheme that includes hail as well as a rain evaporation correction scheme (vs an improved Goddard 3ICE scheme). In addition to the same rain intensity (36) and stratiform fraction bins (20), the LUTs are further differentiated by two new metrics: mean echo top heights (5 bins: 0-2, 2-4, 4-6, 6-8, and above 8 km) and mean low-level (0-2 km) dBZ gradient (increasing or decreasing towards the surface).

Outside the Tropics (i.e., poleward of 37N and 37S), the LH retrievals are based upon a new cold season/ higher latitude algorithm that maps LH profiles based upon 6 NU-WRF (NASA-Unified Weather Research and Forecasting Model) simulations using the same improved 4ICE scheme for 3 eastern US synoptic snow storms and 3 West Coast atmospheric river events. The LUTs are constructed and mapped using the following domain average quantities: storm top heights (6 bins), freezing level (13 bins), max dBZ level (6 bins), dBZ gradient (2 bins), and composite dBZ intensity (90 bins, every 1 dBZ). As with the Tropics, the radar quantities are mean conditional values over each 0.25 x 0.25 degree GPM grid. A radar (composite) coverage factor is then used to scale the corresponding LUT conditional LH profile to obtain the GPM grid average value.

GCE cases for the Revised Tropical LUTs

LUT cases	Type	Location	Period	Duration
ARM 1997	Land	Southern Great Plains	June-July, 1997	29 days
ARM 2002	Land	Southern Great Plains	May-June, 2002	20 days
MC3E	**Land**	**Southern Great Plains**	**April-May, 2011**	**33 days**
GoAMAZON	**Land**	**Amazon Basin**	**Feb-March, 2014**	**40 days**
GATE	Ocean	Tropical Atlantic	Aug-Sept, 1974	20 days
KWAJEX	Ocean	Marshall Islands	July-Sept, 1999	52 days
SCSMEX	Ocean	South China Sea	May-June, 1998	45 days
TOGA COARE	Ocean	Equatorial West Pacific	November, 1992 - February, 1993	120 days
TWPICE	Ocean	Darwin, Australia	Jan-Feb, 2006	6 **(24) days**
DYNAMO	**Ocean**	**Equatorial Indian Ocean**	**Nov-Dec, 2011**	**31 days**

BOLD indicates new additional cases

Table 1

Caveats:

CSH retrievals are derived from Level 2 products from the Combined Radar-Radiometer Algorithm (CMB). Users are encouraged to check related CMB documentation.

CSH retrievals in the tropical TRMM domain are based upon GCE model simulations that do not include terrain. At higher latitudes, the CSH LUTs are based upon NU-WRF simulations that do include terrain. However, areas with domain heights above 500 m were screened out in the construction of the LUTs. Therefore, CSH retrievals both in the Tropics and at higher latitudes in areas with higher terrain should not be relied upon.

Sample Analyses:

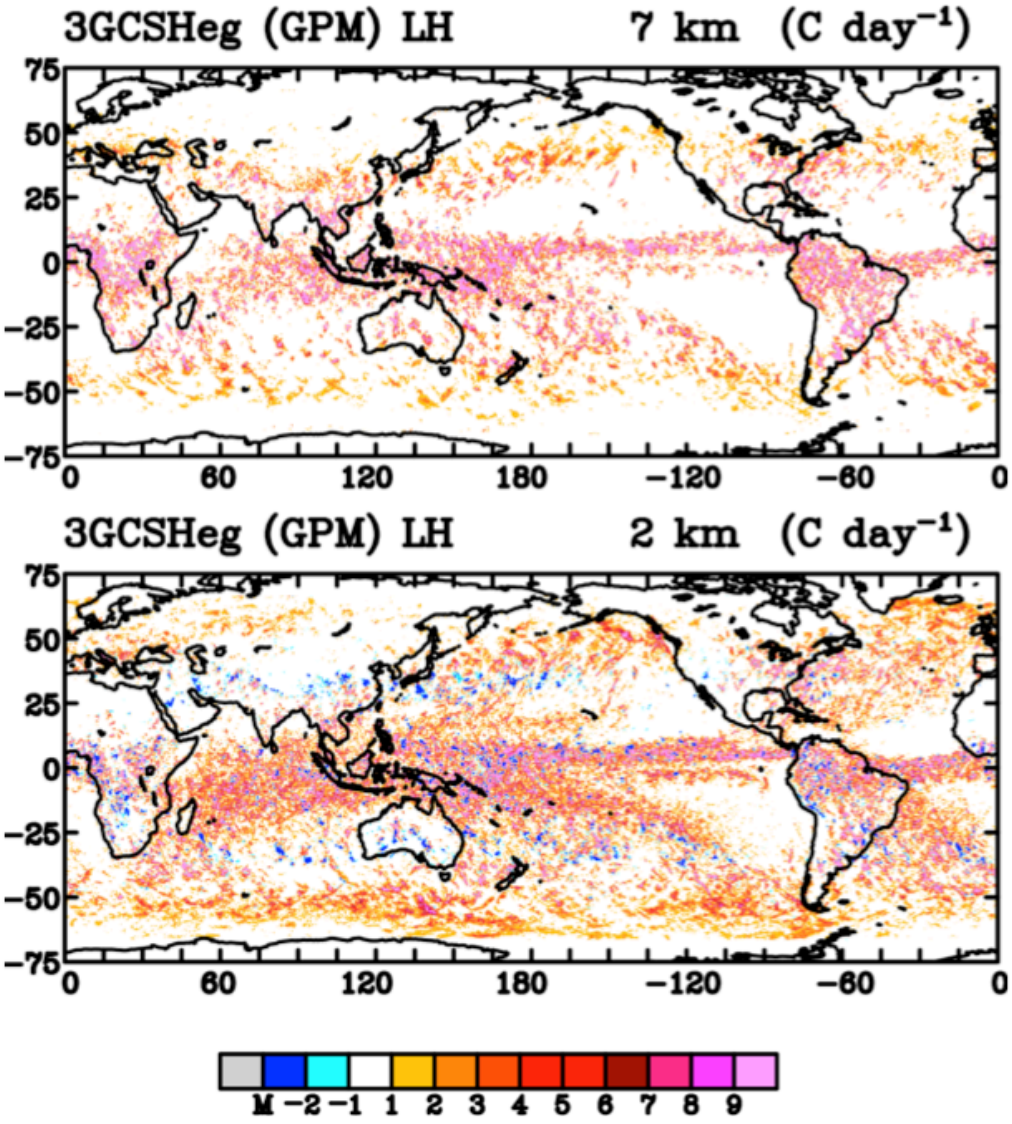

Figure 1. 3GCSH (gridded orbital) V05 LH at 2 and 7 km for April 2014.

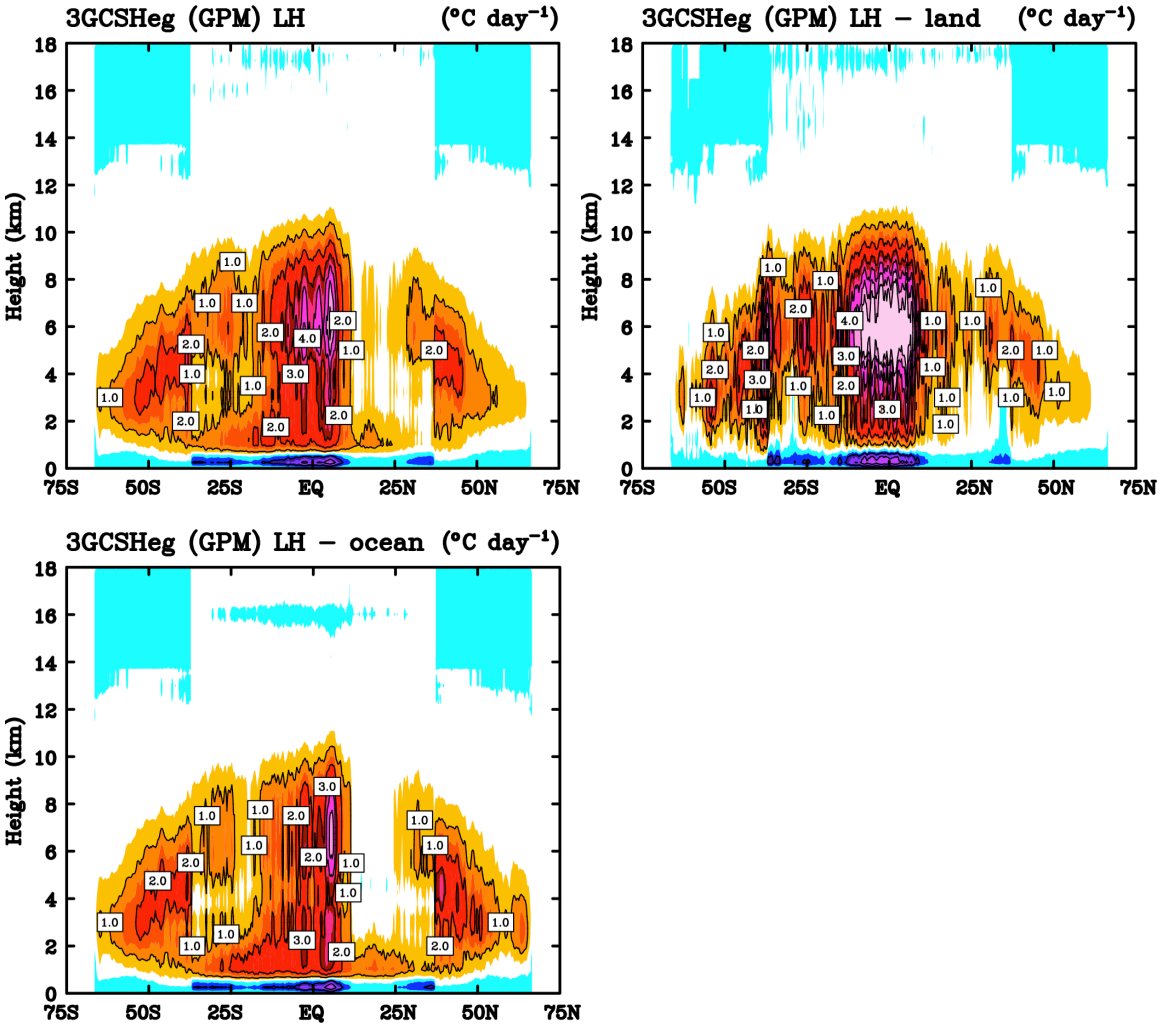

Figure 2. 3GCSH (gridded orbital) V05 zonal average total, land, and ocean LH for April 2014.

References:

Lang, S., W.-K. Tao, J.-D. Chern, D. Wu, and X. Li, 2014: Benefits of a 4th ice class in the simulated radar reflectivities of convective systems using a bulk microphysics scheme. *J. Atmos. Sci.,* **71**, 3583-3612. doi: http://dx.doi.org/10.1175/JAS-D-13-0330.1

Tao, W.-K., S. Lang, X. Zeng, S. Shige, and Y. Takayabu, 2010: Relating convective and stratiform rain to latent heating. *J. Climate.,* **23,** 1874-1893.

Tao, W.-K., D. Wu, S. Lang, J.-D. Chern, C. Peters-Lidard, A. Fridlind, and T. Matsui, 2016: High-resolution NU-WRF simulations of a deep convective-precipitation system during MC3E: Further Improvements and Comparisons between Goddard microphysics schemes and observations. *J. Geophy. Rev. Atmos*., **121**, 1278-1305, doi:10.1002/2015JD023986.

Release Notes for the CSH V05 Level 3 gridded product (3HCSH)

5 July 2017

Changes from V04:

Major changes from V04 include the retrieval of latent heating (LH) over the entire GPM domain (i.e., 67N to 67S), not just the TRMM domain (i.e., 37N to 37S). However, the other remaining CSH products (i.e., eddy heating, microphysical and eddy moistening, and radiation) are still retrieved only over the TRMM domain.

All products are now retrieved at 80 vertical levels every 250 meters AGL starting at the surface (i.e., 0, 250, 500, etc.).

The retrievals for the Tropics (i.e., TRMM domain) are based upon an updated version of the previous CSH algorithm design (Tao et al. 2010). The algorithm still relies upon look-up-tables (LUTs) of model-simulated heating/moistening profiles generated from the Goddard Cumulus Ensemble Model (or GCE), a CRM, which are stored and mapped to satellite grids according to precipitation characteristics. In V04, the previous TRMM V7 CSH LUTs were used. Those LUTs were designed for 0.5 x 0.5 degree TRMM grids (versus the 0.25 x 0.25 degree GPM grids), so the GPM input data in V04 were pre-smoothed to accommodate the coarser resolution of the LUTs. In V05, the LUTs are generated at the GPM grid resolution (0.25 degrees) and are based on 2D multi-week simulations for 6 ocean (vs 5) and 4 land (vs 2) cases (**see Table 1**) using larger domains (512 vs 256 km) and an improved Goddard 4ICE (Lang et al. 2014; Tao et al. 2016) microphysics scheme that includes hail as well as a rain evaporation correction scheme (vs an improved Goddard 3ICE scheme). In addition to the same rain intensity (36) and stratiform fraction bins (20), the LUTs are further differentiated by two new metrics: mean echo top heights (5 bins: 0-2, 2-4, 4-6, 6-8, and above 8 km) and mean low-level (0-2 km) dBZ gradient (increasing or decreasing towards the surface).

Outside the Tropics (i.e., poleward of 37N and 37S), the LH retrievals are based upon a new cold season/ higher latitude algorithm that maps LH profiles based upon 6 NU-WRF (NASA-Unified Weather Research and Forecasting Model) simulations using the same improved 4ICE scheme for 3 eastern US synoptic snow storms and 3 West Coast atmospheric river events. The LUTs are constructed and mapped using the following domain average quantities: storm top heights (6 bins), freezing level (13 bins), max dBZ level (6 bins), dBZ gradient (2 bins), and composite dBZ intensity (90 bins, every 1 dBZ). As with the Tropics, the radar quantities are mean conditional values over each 0.25 x 0.25 degree GPM grid. A radar (composite) coverage factor is then used to scale the corresponding LUT conditional LH profile to obtain the GPM grid average value.

GCE cases for the Revised Tropical LUTs

LUT cases	Type	Location	Period	Duration
ARM 1997	Land	Southern Great Plains	June-July, 1997	29 days
ARM 2002	Land	Southern Great Plains	May-June, 2002	20 days
MC3E	**Land**	**Southern Great Plains**	**April-May, 2011**	**33 days**
GoAMAZON	**Land**	**Amazon Basin**	**Feb-March, 2014**	**40 days**
GATE	Ocean	Tropical Atlantic	Aug-Sept, 1974	20 days
KWAJEX	Ocean	Marshall Islands	July-Sept, 1999	52 days
SCSMEX	Ocean	South China Sea	May-June, 1998	45 days
TOGA COARE	Ocean	Equatorial West Pacific	November, 1992 - February, 1993	120 days
TWPICE	Ocean	Darwin, Australia	Jan-Feb, 2006	6 **(24) days**
DYNAMO	**Ocean**	**Equatorial Indian Ocean**	**Nov-Dec, 2011**	**31 days**

BOLD indicates new additional cases

Table 1

Caveats:

CSH retrievals are derived from Level 2 products from the Combined Radar-Radiometer Algorithm (CMB). Users are encouraged to check related CMB documentation.

CSH retrievals in the tropical TRMM domain are based upon GCE model simulations that do not include terrain. At higher latitudes, the CSH LUTs are based upon NU-WRF simulations that do include terrain. However, areas with domain heights above 500 m were screened out in the construction of the LUTs. Therefore, CSH retrievals both in the Tropics and at higher latitudes in areas with higher terrain should not be relied upon.

References:

Lang, S., W.-K. Tao, J.-D. Chern, D. Wu, and X. Li, 2014: Benefits of a 4th ice class in the simulated radar reflectivities of convective systems using a bulk microphysics scheme. *J. Atmos. Sci.,* **71**, 3583-3612. doi: http://dx.doi.org/10.1175/JAS-D-13-0330.1

Tao, W.-K., S. Lang, X. Zeng, S. Shige, and Y. Takayabu, 2010: Relating convective and stratiform rain to latent heating. *J. Climate.,* **23,** 1874-1893.

Tao, W.-K., D. Wu, S. Lang, J.-D. Chern, C. Peters-Lidard, A. Fridlind, and T. Matsui, 2016: High-resolution NU-WRF simulations of a deep convective-precipitation system during MC3E: Further Improvements and Comparisons between Goddard microphysics schemes and observations. *J. Geophy. Rev. Atmos*., **121**, 1278-1305, doi:10.1002/2015JD023986.